

Equivalence between an optomechanical system and a Kerr medium

Samuel Aldana, Christoph Bruder, and Andreas Nunnenkamp

Department of Physics, University of Basel, Klingelbergstrasse 82, CH-4056 Basel, Switzerland

(Dated: October 24, 2013)

We study the optical bistability of an optomechanical system in which the position of a mechanical oscillator modulates the cavity frequency. The steady-state mean-field equation of the optical mode is identical to the one for a Kerr medium, and thus we expect it to have the same characteristic behavior with a lower, a middle, and an upper branch. However, the presence of position fluctuations of the mechanical resonator leads to a new feature: the upper branch will become unstable at sufficiently strong driving in certain parameter regimes. We identify the appropriate parameter regime for the upper branch to be stable, and we confirm, by numerical investigation of the quantum steady state, that the mechanical mode indeed acts as a Kerr nonlinearity for the optical mode in the low-temperature limit. This equivalence of the optomechanical system and the Kerr medium will be important for future applications of cavity optomechanics in quantum nonlinear optics and quantum information science.

PACS numbers: 42.50.Wk, 42.65.Pc, 37.10.Vz, 85.85.+j

I. INTRODUCTION

Photons are ideal carriers of quantum information [1]. They can propagate large distances in optical fibers before being absorbed, and their polarization has been used for quantum communication and quantum information applications. However, photons barely interact, and thus it is difficult to implement the quantum two-qubit gates needed for universal quantum computation [2]. This situation changes in an optical medium where the photons can inherit an effective interaction, often modeled as a Kerr nonlinearity. This is why so-called Kerr media are important for quantum technology based on photons [3–6].

Recently, it was suggested that optomechanical systems [7] operated in the single-photon strong-coupling regime [8, 9] offer strong effective photon-photon interactions. In optomechanical systems the position of a mechanical oscillator modulates the properties and (most commonly) the frequency of the optical cavity mode. The radiation pressure interaction is intrinsically nonlinear. It induces many interesting effects and enables many applications, e.g. sideband cooling [10, 11], radiation-pressure shot noise [12–15], photon blockade [9], non-Poissonian photon statistics and multiphoton transitions [16], and non-Gaussian and nonclassical mechanical states [8, 17–19].

In this paper, we will focus on the phenomenon of optical bistability, produced by the radiation pressure, and neglect other nonlinear effects such as the photothermal effect [20–22] or a mechanical Duffing nonlinearity. Under certain conditions and sufficiently strong driving there are two classically stable equilibrium positions for the mechanical oscillator and correspondingly for the optical cavity. Optical bistability in optomechanical systems has been discussed in the context of ponderomotive squeezing [23] and entanglement [24], and led to one of the first experimental observations of optomechanical coupling [25, 26]. Optical bistability has also been discussed widely in the context of a Kerr medium [27, 28]. This raises the question whether and in which way the optomechanical system and the Kerr medium in a cavity can be considered to be equivalent, see Fig. 1 that shows both of these systems schematically. In the following we will investigate in detail

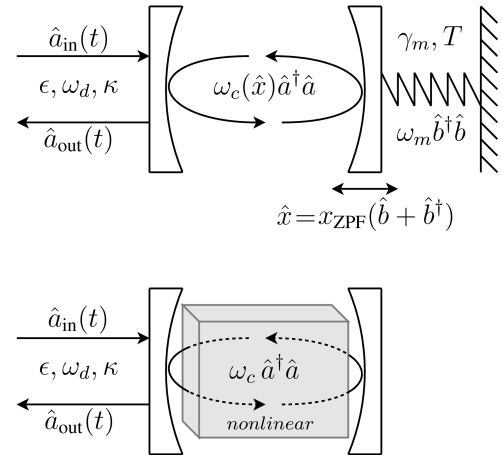


FIG. 1. Optomechanical setup (upper panel) and Kerr medium in a cavity (lower panel). The main part of the paper investigates in detail whether and in which way the two systems are equivalent.

the similarities and differences between optical bistability in an optomechanical system and a Kerr medium.

The paper is organized as follows. In Sec. II we introduce the standard model of optomechanics – a cavity whose frequency is modulated by the position of a mechanical oscillator. We briefly introduce the steady-state mean-field equations of the system and the quantum Langevin description of quantum and thermal fluctuations for a linearized radiation-pressure interaction. In Sec. III we show that the mean-field equation for the optical mode is identical to the one for a Kerr medium, with a lower, a middle and an upper branch. In the optomechanical system, fluctuations of the mechanical mode change the picture. A study of the stability of the different mean-field solutions against fluctuations reveals a feature that is absent from the Kerr medium: the upper branch becomes unstable for certain parameters. We derive conditions on the parameters for this upper branch to remain stable. The stability requires the system to be in the resolved sideband regime with a mechanical quality factor that is not too large. In this case we expect the mechanical resonator to act as an effective Kerr medium for the optical mode, even in the quan-

tum regime. This is confirmed in Sec. IV, where we compare the quantum steady states of both the optomechanical system and the Kerr medium, obtained from numerical solutions of the quantum master equations in the low-temperature limit. The optomechanical system exhibits the expected characteristic quantum signatures proving that it can be regarded as an effective Kerr medium.

II. MODELS FOR THE OPTOMECHANICAL SYSTEM AND THE KERR MEDIUM

We first consider the standard model of optomechanics where the resonance frequency of an optical cavity is modulated by the position of a mechanical resonator (dispersive coupling). A monochromatic coherent light field with frequency ω_d and amplitude ϵ drives the optical mode. The full Hamiltonian, accounting for driving and dissipation, is $\hat{H} = \hat{H}_0 + \hat{H}_d + \hat{H}_\kappa + \hat{H}_{\gamma_m}$, where, in the rotating frame of the driving ($\hbar = 1$),

$$\hat{H}_0 = \omega_m \hat{b}^\dagger \hat{b} - \Delta_0 \hat{a}^\dagger \hat{a} - g_0 \hat{a}^\dagger \hat{a} (\hat{b} + \hat{b}^\dagger), \quad (1)$$

and $\hat{H}_d = i\epsilon(\hat{a} - \hat{a}^\dagger)$. Here, \hat{a} and \hat{b} are the bosonic operators for the optical and mechanical modes, $\Delta_0 = \omega_d - \omega_c$ is the detuning of the drive from the unperturbed cavity resonance frequency ω_c , and ω_m the resonance frequency of the mechanical mode. The optomechanical coupling is given by $g_0 = -x_{\text{ZPF}}(\partial\omega_c/\partial x)$, where $x_{\text{ZPF}} = (2M\omega_m)^{-1/2}$ is the zero-point fluctuation amplitude of the mechanical resonator, M its mass, and $(\partial\omega_c/\partial x)$ is the derivative of the cavity frequency with respect to the resonator position $\hat{x} = x_{\text{ZPF}}(\hat{b} + \hat{b}^\dagger)$. The term \hat{H}_κ describes the damping of the optical cavity at rate κ , and \hat{H}_{γ_m} the damping of the mechanical resonator at rate γ_m . This leads to the definition of two important ratios, the sideband parameter ω_m/κ and the mechanical quality factor $Q_m = \omega_m/\gamma_m$.

Using the input-output formalism [28, 29], the dissipative dynamics of the system is described by the quantum Langevin equations (QLEs)

$$\dot{\hat{a}} = \left(i\Delta_0 - \frac{\kappa}{2}\right) \hat{a} + ig_0 \hat{a} (\hat{b} + \hat{b}^\dagger) - \sqrt{\kappa} \hat{a}_{\text{in}}, \quad (2a)$$

$$\dot{\hat{b}} = -\left(i\omega_m + \frac{\gamma_m}{2}\right) \hat{b} + ig_0 \hat{a}^\dagger \hat{a} - \sqrt{\gamma_m} \hat{\eta}, \quad (2b)$$

where $\hat{a}_{\text{in}}(t) = \bar{a}_{\text{in}} + \hat{\xi}(t)$ consists of a coherent driving amplitude $\bar{a}_{\text{in}} = \epsilon/\sqrt{\kappa}$ and a vacuum noise operator $\hat{\xi}$ which satisfies $\langle \hat{\xi}(t) \hat{\xi}^\dagger(t') \rangle = \delta(t-t')$ and $\langle \hat{\xi}^\dagger(t) \hat{\xi}(t') \rangle = 0$. Similarly, the noise operator $\hat{\eta}$ describes coupling to a Markovian bath at temperature T , i.e., $\langle \hat{\eta}(t) \hat{\eta}^\dagger(t') \rangle = (n_{\text{th}} + 1)\delta(t-t')$ and $\langle \hat{\eta}^\dagger(t) \hat{\eta}(t') \rangle = n_{\text{th}}\delta(t-t')$. In the absence of any other coupling, the bath gives rise to a thermal state with mean occupation number $n_{\text{th}} = [\exp(\omega_m/k_B T) - 1]^{-1}$ for the mechanical oscillator. This treatment of the mechanical dissipation in the form of a QLE for the mechanical amplitude \hat{b} , rather than for the displacement \hat{x} , is correct as long as $Q_m \gg 1$.

The optical and mechanical field operators can be split into a coherent mean-field amplitude and fluctuations: $\hat{a}(t) =$

$\bar{a} + \hat{d}(t)$ and $\hat{b}(t) = \bar{b} + \hat{c}(t)$. Inserting these expressions in the QLEs (2), we obtain two coupled mean-field equations (MFEs) for the amplitudes \bar{a} and \bar{b} . In steady state they read

$$0 = \left[i\Delta_0 + ig_0(\bar{b} + \bar{b}^*) - \frac{\kappa}{2}\right] \bar{a} - \epsilon, \quad (3a)$$

$$0 = -\left(i\omega_m + \frac{\gamma_m}{2}\right) \bar{b} + ig_0 |\bar{a}|^2. \quad (3b)$$

The coherent amplitude of the optical field \bar{a} corresponds to a mean cavity occupation $\bar{n} = |\bar{a}|^2$ and produces a static radiation-pressure force $g_0 \bar{n}/x_{\text{ZPF}}$ on the resonator, displacing its equilibrium position by an amount $x_{\text{ZPF}}(\bar{b} + \bar{b}^*)$. Proceeding this way we eliminate the coherent drive ϵ from the QLEs for the operators \hat{c} and \hat{d} which describe thermal and quantum fluctuations around the mean-field values.

For large optical mean-field amplitudes $|\bar{a}| \gg 1$ and small coupling $g_0 \ll \kappa, \omega_m$, we can neglect the nonlinear terms like $\hat{d}^\dagger \hat{d}$ or $\hat{d} \hat{c}$ in the QLEs. As a result, the optomechanical interaction becomes bilinear: $g_0 \hat{a}^\dagger \hat{a} (\hat{b} + \hat{b}^\dagger) \rightarrow g_0 (\bar{a}^* \hat{d} + \bar{a} \hat{d}^\dagger) (\hat{c} + \hat{c}^\dagger)$. Introducing the convenient vector notation $\hat{\mathbf{u}} = (\hat{d}^\dagger, \hat{d}, \hat{c}^\dagger, \hat{c})^T$ and $\hat{\mathbf{u}}_{\text{in}} = (\sqrt{\kappa} \hat{\xi}^\dagger, \sqrt{\kappa} \hat{\xi}, \sqrt{\gamma_m} \hat{\eta}^\dagger, \sqrt{\gamma_m} \hat{\eta})^T$, we can write the linearized QLEs in matrix form,

$$\frac{d}{dt} \hat{\mathbf{u}}(t) = -\mathbf{A} \cdot \hat{\mathbf{u}}(t) - \hat{\mathbf{u}}_{\text{in}}(t), \quad (4)$$

where \mathbf{A} reads

$$\mathbf{A} = \begin{pmatrix} \frac{\kappa}{2} + i\Delta & 0 & ig^* & ig^* \\ 0 & \frac{\kappa}{2} - i\Delta & -ig & -ig \\ ig & ig^* & \frac{\gamma_m}{2} - i\omega_m & 0 \\ -ig & -ig^* & 0 & \frac{\gamma_m}{2} + i\omega_m \end{pmatrix}. \quad (5)$$

The new parameters entering the matrix \mathbf{A} are the enhanced optomechanical coupling $g = g_0 \bar{a}$ and the effective detuning $\Delta = \Delta_0 + g_0(\bar{b} + \bar{b}^*) = \Delta_0 + 2\bar{n}g_0^2/\omega_m$.

The Kerr medium [27, 28], to which we aim to compare the optomechanical system, is described by the Hamiltonian $\hat{H}' = \hat{H}_K + \hat{H}_d + \hat{H}_\kappa$, where, in the rotating frame of the driving,

$$\hat{H}_K = -\Delta_0 \hat{a}^\dagger \hat{a} - \frac{g_0^2}{\omega_m} (\hat{a}^\dagger \hat{a})^2, \quad (6a)$$

$$\hat{H}_d = i\epsilon(\hat{a} - \hat{a}^\dagger), \quad (6b)$$

and \hat{H}_κ describes again the damping of the optical cavity at rate κ . The QLE for this optical mode \hat{a} is

$$\dot{\hat{a}} = \left[i\left(\Delta_0 + \frac{g_0^2}{\omega_m}\right) - \frac{\kappa}{2}\right] \hat{a} + 2i \frac{g_0^2}{\omega_m} \hat{a}^\dagger \hat{a}^2 - \sqrt{\kappa} \hat{a}_{\text{in}}, \quad (7)$$

where the input operator $\hat{a}_{\text{in}}(t)$ is the same as for the optomechanical system. The steady-state equation for the mean-field amplitude \bar{a} is

$$0 = \left[i\left(\Delta_0 + \frac{g_0^2}{\omega_m}\right) - \frac{\kappa}{2}\right] \bar{a} + 2i \frac{g_0^2}{\omega_m} |\bar{a}|^2 \bar{a} - \epsilon. \quad (8)$$

Replacing Δ_0 by $\Delta_0 - g_0^2/\omega_m$ in Eq. (8) yields the equation for the optical mean-field amplitude \bar{a} of the optomechanical system obtained from Eq. (3) by eliminating the mechanical mean-field amplitude \bar{b} . This frequency shift of the detuning Δ_0 is consistent with the fact that \hat{H}_0 and \hat{H}_K are

connected by the canonical (polaron) transformation $\hat{U} = \exp[(g_0/\omega_m)(\hat{b} - \hat{b}^\dagger)\hat{a}^\dagger\hat{a}]$. Applying \hat{U} to the optomechanical Hamiltonian \hat{H}_0 , Eq. (1), we obtain $\hat{U}\hat{H}_0\hat{U}^\dagger = \hat{H}_K + \omega_n\hat{b}^\dagger\hat{b}$. In this frame, the optomechanical interaction is eliminated and the optical mode acquires a Kerr nonlinearity of the form of Eq. (6a) [8, 9].

III. OPTICAL BISTABILITY IN THE SEMICLASSICAL REGIME

In the following, we will first show that the optomechanical system has MFEs with three solutions in a certain range of driving frequency and driving amplitude, just as the Kerr medium does. After discussing the characteristic behavior of the mean-field solutions in the regime of optical bistability, we study the stability of the mean-field solutions against fluctuations of both the optical and mechanical mode and point out the differences with the Kerr medium. Finally, we find parameters for which the optomechanical system is accurately described by an effective Kerr medium.

A. Bistability at the mean-field level

We briefly review the origin of bistability in the mean-field equations of the optomechanical system [23, 26, 30, 31].

To simplify the notation we define the dimensionless nonlinearity parameter χ , detuning y , and driving power z by

$$\begin{aligned}\chi &= \frac{g_0^2}{\omega_m\kappa}, \\ y &= -\frac{\Delta_0}{\kappa}, \\ z &= \chi \left(\frac{\epsilon}{\kappa}\right)^2.\end{aligned}$$

Combining Eqs. (3a) and (3b) we obtain a third-order polynomial root equation for the mean-field cavity occupation, $p(\chi\bar{n}) = 0$, where

$$p(\lambda) = 4\lambda^3 - 4y\lambda^2 + \left(y^2 + \frac{1}{4}\right)\lambda - z. \quad (9)$$

The MFE for the Kerr medium, Eq. (8), leads to the same equation for \bar{n} , provided we replace y by $y - \chi$ in Eq. (9).

Equation (9) indicates that the MFEs can have either one or three solutions, depending on the number of real roots of the polynomial. The three roots depend on the dimensionless detuning y and driving power z . Since the mean-field cavity occupation \bar{n} follows from $p(\chi\bar{n}) = 0$, the nonlinearity parameter χ determines whether optical bistability occurs at small or large driving power and photon number.

The optical mean-field amplitude is $\bar{a} = -e^{i\varphi}\sqrt{\lambda/\chi}$, where $\varphi = \arctan(4\lambda - 2y)$. If the detuning y and driving power z are such that the equation $p(\lambda) = 0$ has three real roots, the smaller χ , the more distant in phase space are the different optical mean-field amplitudes \bar{a} . A similar observation can be made concerning the mechanical resonator: the

equation $p(\lambda) = 0$ also holds for $\lambda = \sqrt{\chi\omega_m/(4\kappa)}(\bar{b} + \bar{b}^*)$, where $\bar{b} + \bar{b}^*$ is the equilibrium position of the mechanical resonator in units of x_{ZPF} . Therefore, the smaller χ and the sideband parameter ω_m/κ , the more distant are the different equilibrium positions.

We now examine some characteristic features of the MFEs, which occur both in an optomechanical system (3) and a Kerr medium (8). To this end, we find the conditions on the detuning y and the driving power z for the MFEs to have three solutions, and illustrate them with a few examples.

First we observe that the equation $p(\lambda) = 0$ can have three real roots only if the detuning y and the driving power z exceed some threshold value \tilde{y} and \tilde{z} [23, 32],

$$y > \tilde{y} = \frac{\sqrt{3}}{2} \simeq 0.87, \quad (10a)$$

$$z > \tilde{z} = \frac{1}{6\sqrt{3}} \simeq 0.1. \quad (10b)$$

Therefore, optical bistability can only be found for red-detuned driving frequencies. In addition, the three roots are real only if

$$z_-(y) < z < z_+(y), \quad (11)$$

where

$$z_{\pm}(y) = \frac{1}{27} \left[y(y^2 + 3\tilde{y}^2) \pm (y^2 - \tilde{y}^2)^{3/2} \right].$$

The region in (y, z) -parameter space where Eqs. (10) and (11) are satisfied is shown in Fig. 2(c) with the labels *II* (blue) and *III* (purple). In this region the three mean-field occupations satisfy $\bar{n}_1 < n_- < \bar{n}_2 < n_+ < \bar{n}_3$, where n_{\pm} are found from $p'(\chi n_{\pm}) = 0$ and read

$$\chi n_{\pm}(y) = \frac{1}{6} \left[2y \pm (y^2 - \tilde{y}^2)^{1/2} \right]. \quad (12)$$

In the following, we refer to \bar{n}_1 , \bar{n}_2 , and \bar{n}_3 as the lower, middle, and upper branch of the MFEs.

In Fig. 2(a) we show the mean-field occupation $\chi\bar{n}$ as a function of the driving power z for fixed detuning y . For an increasing driving power z and a detuning above the threshold $y > \tilde{y}$, the three branches of the mean-field occupation \bar{n} form a characteristic *S*-shaped curve. The lower branch starts from the origin and ends at the turning point given by (z_+, n_-) where the middle branch starts. The upper branch starts from the second turning (z_-, n_+) , where the middle branch ends, and increases further.

In Fig. 2(b) we plot the mean-field occupation $\chi\bar{n}$ as a function of the detuning y for fixed driving power z . The cavity line shape is approximately Lorentzian if the driving power is far below the threshold $z \ll \tilde{z}$ (not shown). For larger and larger z it becomes more and more asymmetric and tilts until for $z = \tilde{z}$, it has an infinite slope at $y = \tilde{y}$. For a driving power beyond this threshold the cavity line-shape has three branches in the range of detuning y determined by Eq. (11).

According to these considerations, the optomechanical system and the Kerr medium are equivalent at the level of the steady-state MFEs. Our next goal is to discuss the stability of

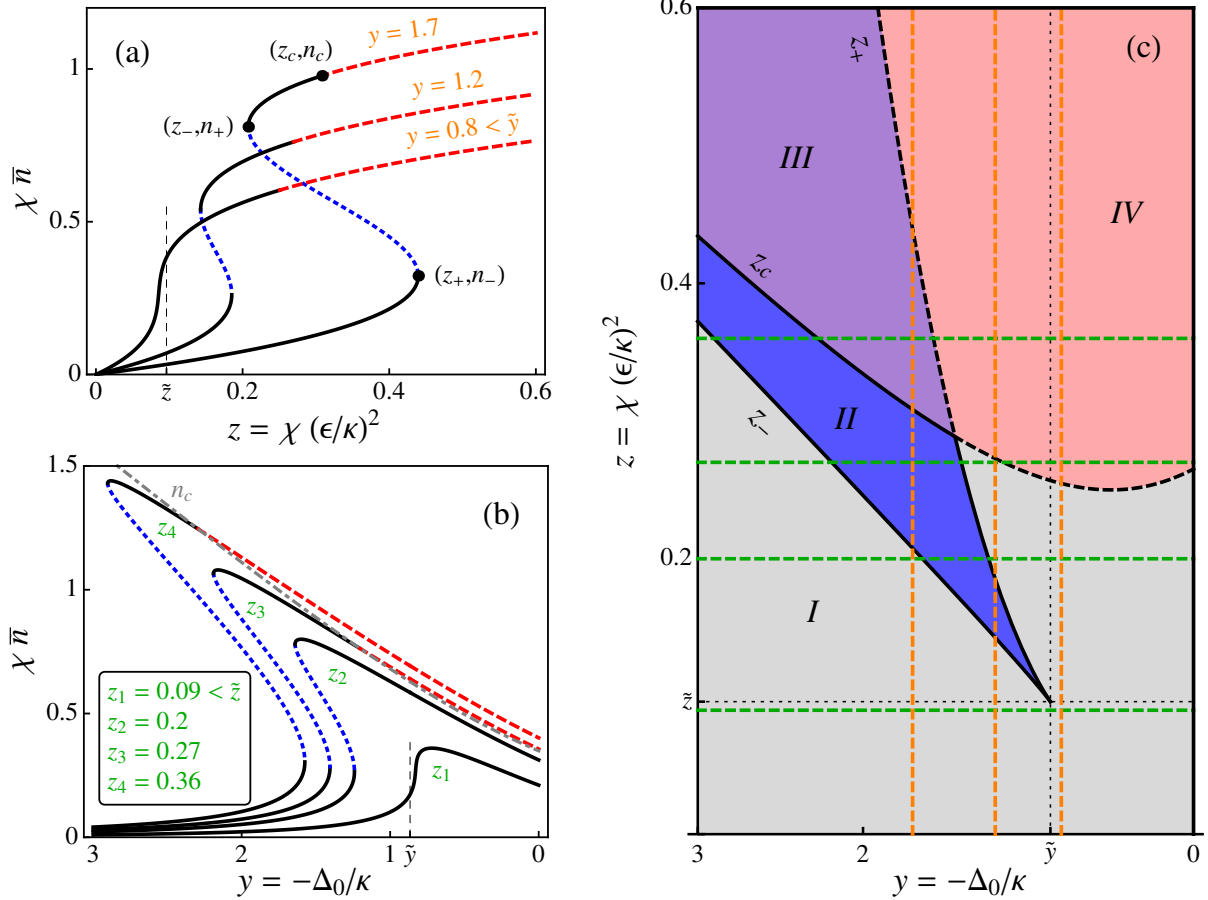


FIG. 2. (Color online) *Optical bistability in the semiclassical regime.* Typical curves for the mean-field cavity occupation \bar{n} as a function of the dimensionless driving power z (a) and the dimensionless detuning y (b), obtained from the condition $p(\chi\bar{n}) = 0$ [see Eq. (9)]. According to the stability criteria $c_{1,2} > 0$ [see Eqs. (13)], Gaussian fluctuations lead to stable (solid black) or unstable (dotted blue and dashed red) mean-field solutions. As in the case of the Kerr medium, the first criterion $c_1 > 0$ always yields an unstable middle branch (dotted blue), while the additional criterion for the optomechanical system $c_2 > 0$ can turn part of the upper or only branch unstable (dashed red). In (b) we also show the critical mean-field occupation n_c (dash-dotted gray) obtained from the condition $c_2 = 0$. In (c) we summarize the behavior of the mean-field solution as a function of the parameters y and z . In regions II and III, between the curves z_- and z_+ , Eqs. (10) and (11) are satisfied and there are three distinct mean-field solutions; the middle branch is always unstable. In region II (blue) the lower and upper branches are stable. In region III (purple) the second stability criterion shows the upper branch to be unstable ($c_2 < 0$) and only the lower branch is stable. In regions I and IV the mean-field equations (MFEs) have only one solution. Below the z_c curve in region I (gray) this unique branch is stable, while in region IV (red) the second criterion again shows that this solution is unstable ($c_2 < 0$). The values of the detuning y and driving power z used in (a) and (b) are indicated by the orange and green dashed lines. Note that none of these features depends on the nonlinearity parameter χ , due to appropriate scaling of the axes. The threshold detuning \tilde{y} and driving power \tilde{z} indicate the minimal values of y and z needed for the MFEs to have three solutions. The sideband parameter and mechanical quality factor chosen to show the influence of the second stability criterion $c_2 > 0$ are $\omega_m/\kappa = 10$ and $Q_m = 1000$.

the different branches of the MFEs. The existence of three solutions to the MFEs indicates that the optomechanical system may be in a regime of bistability, with stable lower and upper branches, as well as an unstable middle branch. While for the Kerr medium this is always true [27], a stability analysis leads to different conclusions in the case of the optomechanical system. In addition, if the detuning y and driving power z lead to a unique solution for the mean-field cavity occupation \bar{n} , this solution is always stable for the Kerr medium, but not necessarily so for the optomechanical system.

B. Stability analysis of the mean-field solutions

The upper and lower branches are always stable for the Kerr medium. To find the range of parameters where the optomechanical system reproduces this behavior, we analyze the stability of the different branches of the MFEs (3) against fluctuations of both the optical and mechanical modes.

The stability of a point in any of the branches of the MFEs is established, if the linear QLEs (4), describing the fluctuations around this point, are stable. This in turn is ensured if all the eigenvalues of the matrix A given in Eq. (5), derived from the

corresponding mean-field amplitudes \bar{a} and \bar{b} , have positive real parts. This has to be verified even if the MFEs have only one solution.

The differences and similarities between the optomechanical system and the Kerr medium are summarized in Table I.

TABLE I. Stability for the different branches in an optomechanical system and a Kerr medium determined from the QLEs (4) and (7). The critical mean-field occupation n_c is found from the stability criterion, Eq. (13b), and depends on the detuning $y = -\Delta_0/\kappa$, the sideband parameter ω_m/κ , and the mechanical quality factor Q_m .

Branch #	type	Kerr medium	Optomechanical system	
3	lower	stable	stable	
	middle	unstable	unstable	
	upper	stable	stable $\bar{n} < n_c$	unstable $\bar{n} > n_c$
1	-	stable	stable $\bar{n} < n_c$	unstable $\bar{n} > n_c$

The difference between the two systems is explained by the parametric instability in the optomechanical system [33, 34] that occurs at a mean-field occupation \bar{n} above some critical value n_c . Around such a mean-field solution, the linear dynamics of optical and mechanical fluctuations becomes unstable. This particular feature of the optomechanical system is illustrated in Fig. 2; it is absent for the Kerr medium.

In Figs. 2(a) and 2(b), we indicate the unstable segments of the branches where $\bar{n} > n_c$. In case the MFEs have three branches, this critical value for the mean-field occupation n_c systematically lies in the upper branch or in its extension to the region where there is only one branch.

In Fig. 2(a), for a fixed detuning above threshold $y > \tilde{y}$, the upper branch is stable only in a finite segment near the second turning point n_+ at the beginning of the upper branch. The size of this stable segment diminishes as the detuning y increases, and shrinks to a single point in the limit of a far red-detuned driving frequency. The same effect is seen in Fig. 2(b). With increasing driving power z the stability in the upper branch is confined to a smaller and smaller segment near the maximum of the cavity line shape.

In Fig. 2(c), the regions in (y, z) -parameter space where the upper or only branch turns unstable are labeled by III and IV. These are the regions where the driving power z is larger than the critical value z_c , found by solving the equation $p(\chi n_c) = 0$ for z , where p is given in Eq. (9). The range of detuning y or driving power z at which bistability is observed shrinks with increasing y or z .

We now characterize the regime leading to optical bistability in the optomechanical system, and therefore examine how the stability of the branches depends on the parameters. To this end, we apply the Routh-Hurwitz criterion to the linear QLEs (4). Two conditions have to be satisfied for a particular

mean-field solution to be stable, $c_{1,2} > 0$, where [35]

$$c_1 = 4|g|^2\Delta + \omega_m \left(\Delta^2 + \frac{\kappa^2}{4} \right), \quad (13a)$$

$$c_2 = \kappa \gamma_m \left[(\Delta^2 - \omega_m^2)^2 + \frac{1}{2} (\Delta^2 + \omega_m^2) (\kappa + \gamma_m)^2 + \frac{1}{16} (\kappa + \gamma_m)^4 \right] - 4|g|^2\Delta \omega_m (\kappa + \gamma_m)^2. \quad (13b)$$

The identification of the parameter regime leading to $c_{1,2} > 0$ is done as follows. We replace $|g|^2$ and Δ by their \bar{n} -dependent expressions,

$$|g|^2 = \kappa \omega_m \chi \bar{n}, \\ \Delta = \kappa(2\chi \bar{n} - y),$$

in Eqs. (13), and express $c_{1,2}$ as functions of the rescaled mean-field occupation $\chi \bar{n}$, the detuning y , the sideband parameter ω_m/κ , and the mechanical quality factor $Q_m = \omega_m/\gamma_m$.

From the condition $c_1 < 0$ we conclude that the middle branch is unstable [23, 30, 31]. This follows from $\text{sgn}(c_1) = \text{sgn}[(n_+ - \bar{n})(n_- - \bar{n})]$, where n_{\pm} , Eq. (12), are the values of the mean-field cavity occupation at the lower and upper limits of the middle branch. The physical interpretation of this condition is simple. In the middle branch, the modification of the mechanical frequency due to radiation pressure, also known as the optical spring effect, is such that the modified mechanical force is no longer a restoring force.

In the Kerr medium, the same stability condition, $c_1 > 0$, is found from the linear QLEs, obtained by substituting $\hat{a} = \bar{a} + \hat{d}$ in Eq. (7) and neglecting second- and third-order terms in \hat{d} , \hat{d}^\dagger . No other criteria are needed to establish the stability of the system, and therefore the lower and upper branches are always stable.

The condition $c_2 = 0$ is equivalent to the relaxation rate of the system going to zero [36]. In a stable system, this relaxation rate is the real part of the eigenvalue of \mathbf{A} closest to zero. Above the critical mean-field occupation, $\bar{n} > n_c$, this relaxation rate becomes negative, $c_2 < 0$, and the branch turns unstable. If in addition \bar{n} is the only mean-field solution, the system is parametrically unstable. We find n_c by solving the equation $c_2 = 0$ for \bar{n} , as a function of the detuning y , the sideband parameter ω_m/κ , and the mechanical quality factor Q_m .

It turns out that n_c always lies in the upper branch or in its extension to the region with only one branch. This can be seen as follows. Since the condition $c_2 > 0$ is automatically satisfied for negative *effective* detuning, $\Delta \leq 0$, we find a lower bound for the critical occupation,

$$n_c \geq n_\Delta = \frac{y}{2\chi}.$$

In addition, the effective detuning Δ always turns positive in the upper branch, since $n_\Delta \geq n_+$. Thus the upper branch is only stable in the range $n_+ < \bar{n} < n_c$. This stable portion can be very small, e.g., in the extreme case $-\Delta_0 \gg \kappa$ and $\gamma_m = 0$, we have $n_c = n_\Delta \simeq n_+$.

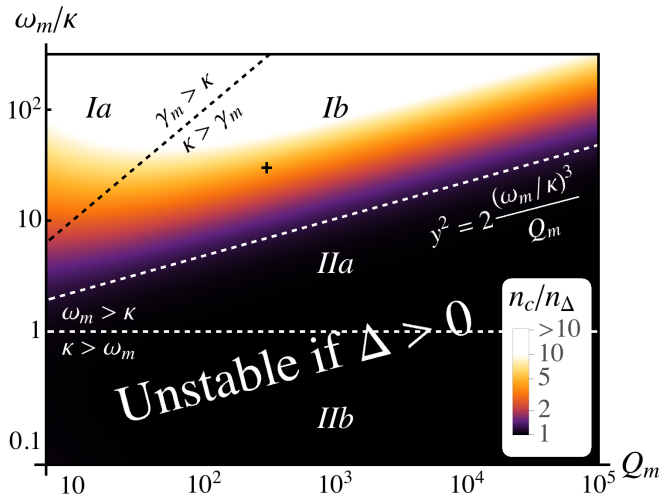


FIG. 3. (Color online) Critical cavity occupation n_c in units of n_Δ , as a function of the sideband parameter ω_m/κ and the mechanical quality factor Q_m . At n_c the mean-field solution \bar{n} leads to unstable linear dynamics for the optomechanical system. The cavity occupation $n_\Delta = y/(2\chi)$ marks the point at which the effective detuning Δ becomes positive. We find n_c from the second stability criterion, Eq. (13b). The bare detuning is $y = -\Delta_0/\kappa = 1.5$. Note that the ratio n_c/n_Δ does not depend on the nonlinearity parameter χ . The black cross indicates the parameters used in Fig. 4.

In Fig. 3 we compare the critical mean-field cavity occupation n_c to the occupation n_Δ at which Δ changes sign. The ratio n_c/n_Δ is shown as a function of ω_m/κ and Q_m . If n_c/n_Δ is large, the upper branch is stable beyond the parameter range leading to bistability, $n_c \gg n_+$, mimicking the behavior of the Kerr medium. On the contrary, if $n_c/n_\Delta \simeq 1$, the upper branch turns unstable for $\Delta > 0$ and is only stable on a finite segment near its beginning.

We can distinguish four parameter regimes which encompass most experimental situations.

1. Resolved sideband and large mechanical damping (Ia)

For extremely low cavity damping, $\omega_m > \gamma_m > \kappa$, the critical occupation n_c is approximately

$$\chi n_c = \frac{1}{4} \left(y + \sqrt{y^2 + 2 Q_m \frac{\omega_m}{\kappa}} \right).$$

In the case of a fixed detuning satisfying $y^2 \ll 2 Q_m \omega_m/\kappa$, we have $n_c \gg n_\Delta$ and the upper branch is stable on a considerable segment, extending up to driving powers z and mean-field occupations \bar{n} that are much larger than those needed for bistable MFEs, i.e., $z_c \gg z_+$ and $n_c \gg n_+$. We recall that z_c is found by solving the equation $p(\chi n_c) = 0$, with p defined in Eq. (9). Therefore, the mean-field behavior of the optomechanical system is equivalent to the behavior of a Kerr medium in the regime of bistability. In Ref. 16, the optomechanical system was compared to the Kerr medium in terms of the full counting statistics of photons. Although the two systems can behave differently in some regime of parameters, the

authors demonstrate that the influence of the mechanical resonator reduces to an effective Kerr nonlinearity when $\gamma_m \sim \kappa$, in particular with $y = \omega_m/\kappa$.

2. Resolved sideband and small mechanical damping (Ib and IIa)

In the regime characterized by $\omega_m > \kappa > \gamma_m$, the critical mean-field cavity occupation is found to be approximately

$$\chi n_c = \frac{1}{4} \left(y + \sqrt{y^2 + 2 \frac{(\omega_m/\kappa)^3}{Q_m}} \right). \quad (14)$$

In this case, the parameter $(\omega_m/\kappa)^3/Q_m$ plays an important role to characterize the mean-field behavior.

If $Q_m > (\omega_m/\kappa)^3$, we obtain $n_c \simeq n_\Delta$ for a detuning above the bistability threshold $y > \tilde{y}$. In this case, the upper branch turns unstable if the effective detuning is positive, $\Delta > 0$. In addition, this means that if the detuning is negative and large, such that $-\Delta_0 \gg \kappa$, the stable segment is small, as $n_\Delta \simeq n_+$.

In the opposite limit, $Q_m \ll (\omega_m/\kappa)^3$, we can have $n_c \gg n_\Delta$ as in the previous case ($\gamma_m > \kappa$), provided the detuning y satisfies $y^2 \ll (\omega_m/\kappa)^3/Q_m$. The same conclusions then apply, i.e., $z_c \gg z_+$ and $n_c \gg n_+$, and the mean-field behavior of the optomechanical system and the Kerr medium is equivalent in the parameter regime of bistability.

Using the exact expression for n_c , we see in Fig. 3 that the border between the region where the optomechanical system experiences a parametric instability as soon as $\Delta > 0$ (black region), and the region where the system is still linearly stable for some positive effective detuning, $n_c > n_\Delta$, is approximately given by $y^2 = 2(\omega_m/\kappa)^3/Q_m$. Above this line, an optomechanical system driven to the regime of bistability behaves like a Kerr medium, as described by Eqs. (6) and (7). This will be confirmed in the next section by obtaining the quantum steady state of both systems numerically and showing that the states of the optical mode are similar.

Many experimental realizations of cavity optomechanics are in the resolved-sideband limit and fall into this category [39]: micromechanical microwave resonators [40–43], coated micromechanical resonators [44], photonic crystal cavities [45], microspheres [46], and microtoroids [47, 48].

3. Unresolved sideband and small mechanical damping (IIb)

The critical occupation n_c can be approximated in the limit of a small sideband parameter ω_m/κ and large enough mechanical quality factor, such that $1 > \omega_m/\kappa > 1/Q_m$, as

$$\chi n_c = \frac{1}{4} \left(y + \sqrt{y^2 + \frac{\kappa/\omega_m}{8 Q_m}} \right). \quad (15)$$

If the bare detuning Δ_0 is negative and exceeds the threshold value for possible bistability, $y > \tilde{y}$, we obtain that $n_c \simeq n_\Delta$. The upper branch turns unstable as soon as the effective detuning Δ is positive, and for large bare red detuning, $-\Delta_0 \gg \kappa$,

the upper branch is only stable on a small segment close to its beginning.

In this regime we find several experimental implementations of optomechanics: ultracold atoms [49–51], suspended membranes [52], and coated mechanical resonators [53, 54].

A simple interpretation of the critical mean-field occupation n_c in Eqs. (14) and (15) can be provided by considering the total mechanical damping $\gamma_{\text{tot}} = \gamma_m + \Gamma_{\text{opt}}$, where Γ_{opt} is the additional mechanical damping induced by coupling to the optical degree of freedom. In the weak-coupling limit of linearized optomechanics, i.e., $g, \gamma_m < \kappa$, this contribution is given by $\Gamma_{\text{opt}} = -2 \text{Im} \Sigma(\omega_m)$ where $\Sigma(\omega) = -ig^2 [\chi_c(\omega) - \chi_c^*(-\omega)]$ is the so-called optomechanical self-energy and $\chi_c(\omega) = [\kappa/2 - i(\Delta + \omega)]^{-1}$ the optical susceptibility [11]. In this case, the condition $\bar{n} = n_c$ coincides with $\gamma_{\text{tot}} = 0$ in both limits $\omega_m \lesssim \kappa$.

4. Very small sideband parameter

In the regime where the sideband parameter is so small that $\omega_m/\kappa \ll 1/Q_m$, the situation is different. The upper branch is unconditionally stable as long as the detuning y is not too large, $y < \kappa/(\sqrt{32}Q_m\omega_m)$. For larger values of y , an unstable segment of the upper branch develops, from the second turning point n_+ up to some value n' of the mean-field cavity occupation given by

$$\chi n' = y \left(\frac{1}{2} + Q_m \frac{\omega_m}{\kappa} + \sqrt{\left(Q_m \frac{\omega_m}{\kappa} \right)^2 - \frac{1}{32y^2}} \right).$$

The dynamical timescales of the two modes are different in this limit. The optical mode adiabatically follows the mechanical motion and produces an effective mechanical potential with two stable equilibrium positions. However, as we have seen in the previous paragraph, this picture holds only if Q_m is not too large compared to κ/ω_m .

In this parameter regime, early experiments with hertz-scale mechanical resonance frequencies enabled the first observations of optical bistability and the related hysteresis cycle both in the optical [25] and the microwave domain [26].

In low-finesse cavities, the optical field can create several stable minima in the mechanical potential, a phenomenon sometimes referred to as multistability [30, 31]. It has recently been observed with a torsion balance oscillator acting as the moving mirror [55]. This effect should not be confused with *dynamical* multistability [33], where mechanical limit-cycle orbits of stable amplitudes arise due to parametric instability.

IV. OPTICAL BISTABILITY IN THE QUANTUM REGIME

So far we have focused on the semiclassical regime, considering the mean-field solutions as well as the effect of fluctuations around them, and have identified the regime of parameters where the optomechanical system and the Kerr medium exhibit similar behavior. In the remainder, we want to confirm

that the conclusions of this approach also hold in the quantum limit. To this end, we compare the quantum steady states of the optomechanical system and the Kerr medium, obtained from numerical solutions of the quantum master equations.

A. Quantum master equations description of dissipation

An alternative description of either the optomechanical system or the Kerr medium can be given in the form of quantum master equations, which describe the dynamics of their density operators $\hat{\rho}$, respectively $\hat{\rho}_K$. This treatment is equivalent to the quantum Langevin description given by Eqs. (2) and (7). Instead of using input noise operators $\hat{\xi}$ or $\hat{\eta}$, dissipation is taken into account with Lindblad dissipative terms.

The quantum master equation for the optomechanical system reads

$$\begin{aligned} \frac{d\hat{\rho}}{dt} = \mathcal{L}[\hat{\rho}] = & -i \left[\hat{H}_0 + \hat{H}_d, \hat{\rho} \right] + \kappa \mathcal{D}_{\hat{a}}[\hat{\rho}] \\ & + (n_{\text{th}} + 1)\gamma_m \mathcal{D}_{\hat{b}}[\hat{\rho}] + n_{\text{th}}\gamma_m \mathcal{D}_{\hat{b}^\dagger}[\hat{\rho}], \end{aligned} \quad (16)$$

where the dissipative terms have the standard form, $\mathcal{D}_{\hat{o}}[\hat{\rho}] = \hat{o}\hat{\rho}\hat{o}^\dagger - \frac{1}{2}(\hat{o}^\dagger\hat{o}\hat{\rho} + \hat{\rho}\hat{o}^\dagger\hat{o})$.

In the same way, the quantum master equation for the equivalent Kerr medium is given by

$$\frac{d\hat{\rho}_K}{dt} = \mathcal{L}_K[\hat{\rho}_K] = -i \left[\hat{H}_K + \hat{H}_d, \hat{\rho}_K \right] + \kappa \mathcal{D}_{\hat{a}}[\hat{\rho}_K]. \quad (17)$$

The steady-state density operators are found from the numerical solutions of $\mathcal{L}[\hat{\rho}] = 0$ and $\mathcal{L}_K[\hat{\rho}_K] = 0$, respectively.

B. Comparison of the quantum steady states

To corroborate the fact that the optomechanical system behaves like an effective Kerr medium, we compare the quantum steady states of both systems for parameters that lead to bistable behavior. To this end, we calculate the photon number $\langle \hat{a}^\dagger \hat{a} \rangle$, the cavity amplitude $|\langle \hat{a} \rangle|^2$, and the second-order correlation function

$$g^{(2)}(0) = \frac{\langle \hat{a}^\dagger \hat{a}^\dagger \hat{a} \hat{a} \rangle}{\langle \hat{a}^\dagger \hat{a} \rangle^2},$$

which describes fluctuations in the photon number. We also characterize the similarity between the optomechanical system and the Kerr medium with the help of the overlap

$$F(\hat{\rho}_{\text{opt}}, \hat{\rho}_K) = \text{Tr} \left[\sqrt{\sqrt{\hat{\rho}_K} \hat{\rho}_{\text{opt}} \sqrt{\hat{\rho}_K}} \right], \quad (18)$$

where $\hat{\rho}_{\text{opt}}$ is the reduced density matrix of the system, obtained by tracing out the mechanical degree of freedom from $\hat{\rho}$. Finally, we investigate the Wigner distribution function of the optical mode, which reads

$$W_{\text{opt}}(\alpha) = \frac{1}{\pi^2} \int d^2\lambda \text{Tr} \left[\hat{\rho}_{\text{opt}} e^{\lambda(\hat{a}^\dagger - \alpha^*) - \lambda^*(\hat{a} - \alpha)} \right].$$

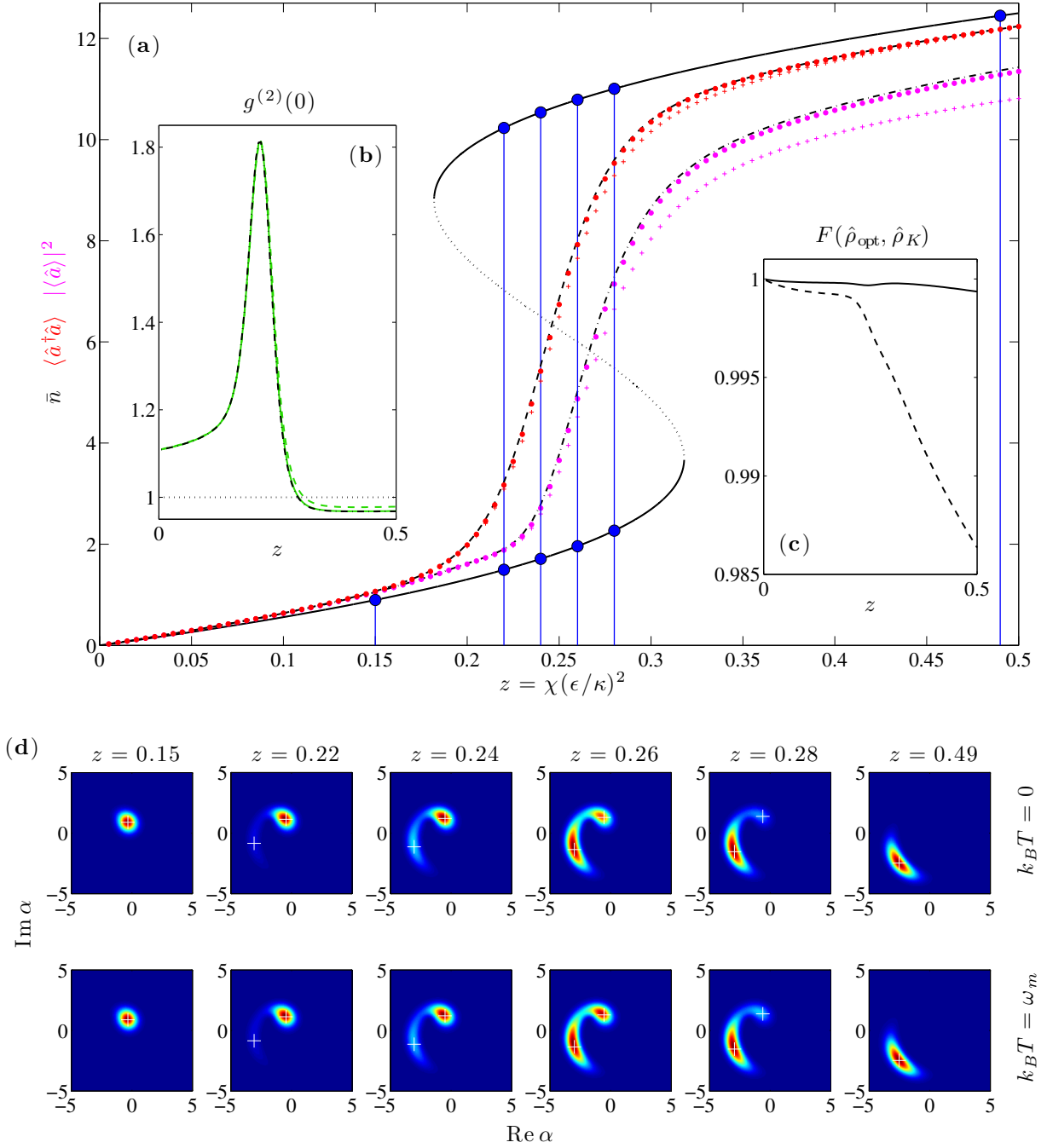


FIG. 4. (Color online) *Optical bistability in the quantum regime.* (a) Mean-field cavity occupation \bar{n} , with stable (black solid line) and unstable (black dotted line) branches, steady-state photon number $\langle \hat{a}^\dagger \hat{a} \rangle$ (red), and cavity amplitude $|\langle \hat{a} \rangle|^2$ (purple) of the optomechanical system, as a function of the dimensionless driving power z . The upper branch turns unstable outside the range of z parameters we plot, beyond $z_c \simeq 92$ and $n_c \simeq 42$. For comparison we also show $\langle \hat{a}^\dagger \hat{a} \rangle$ (black dashed line) and $|\langle \hat{a} \rangle|^2$ (black dash-dotted line) for the equivalent Kerr medium. For both systems, $y = -\Delta_0/\kappa = 1.5$ and $\chi = 0.08$. The parameters of the optomechanical system are $\omega_m/\kappa = 30$, $Q_m = 300$ (indicated by the black cross in Fig. 3), and $k_B T = 0$ (dots) or $k_B T = \omega_m$ (crosses). Inset (b) shows the second-order correlation function $g^{(2)}(0) = \langle \hat{a}^\dagger \hat{a}^\dagger \hat{a} \hat{a} \rangle / \langle \hat{a}^\dagger \hat{a} \rangle^2$ for the optomechanical system with $k_B T = 0$ (green solid line) as well as $k_B T = \omega_m$ (green dashed line) and for the Kerr medium (black dash-dotted line). The first and third curves are indistinguishable. Inset (c) shows the overlap $F(\hat{\rho}_{\text{opt}}, \hat{\rho}_K)$, as defined in Eq. (18), between the density matrices of the pure Kerr medium $\hat{\rho}_K$ and the reduced density matrix of the optomechanical system $\hat{\rho}_{\text{opt}}$, obtained by tracing out the mechanical degree of freedom from $\hat{\rho}$. The temperatures chosen are $k_B T = 0$ (solid line) and $k_B T = \omega_m$ (dashed line). (d) Wigner function $W_{\text{opt}}(\alpha)$ of the optical mode of the optomechanical system for six different driving powers z and two different temperatures. The white crosses indicate the mean-field amplitudes \bar{a} of the stable branches. The values of z are indicated by blue dots and lines in (a).

The steady states of both systems are compared for a constant detuning above the bistability threshold, $y > \tilde{y}$, and as a function of the driving power z . In this configuration the mean-field cavity occupation \bar{n} forms a characteristic S -shaped curve.

The results are presented in Fig. 4. In the upper panel, we show the mean-field cavity occupation \bar{n} , the photon number $\langle \hat{a}^\dagger \hat{a} \rangle$, and the cavity amplitude $|\langle \hat{a} \rangle|^2$ for both the optomechanical system, with zero and finite temperature of the mechanical bath, as well as for the equivalent Kerr medium. The two insets show the second-order correlation $g^{(2)}(0)$ and the overlap $F(\hat{\rho}_{\text{opt}}, \hat{\rho}_K)$. The lower panel of Fig. 4 shows the optical Wigner density function of the optomechanical system.

At low driving power before entering the region of bistability, $z < z_-$, the state of the optical mode is rather well described by a coherent state in both systems, as $\langle \hat{a}^\dagger \hat{a} \rangle = |\langle \hat{a} \rangle|^2 \simeq \bar{n}$.

In the range of driving power where two stable mean-field solutions exist, $z_- < z < z_+$, the master equations (16) and (17) have *unique* quantum steady states. Thus, instead of any bistable behavior, a transition of $\langle \hat{a}^\dagger \hat{a} \rangle$ and $|\langle \hat{a} \rangle|^2$, from the lower to the upper branch, occurs, as the driving power z increases. Simultaneously, both systems show large fluctuations in the photon number, $g^{(2)}(0) > 1$. Such behavior, in the regime where the MFEs lead to bistability, is well-known from the Kerr medium [27].

In this regime, the Wigner function $W_{\text{opt}}(\alpha)$, shown in the lower part of Fig. 4, exhibits two separate lobes peaked at the mean-field amplitudes, $\alpha \simeq \bar{a}$. This is another well-known feature of the Kerr medium [32, 56] and shows how classical bistability persists in the quantum regime. The two lobes are distinguishable if the phase-space separation of the two stable mean-field amplitudes \bar{a} is larger than the fluctuations around them, which is satisfied here since $\chi \ll 1$. Since $W_{\text{opt}} > 0$ everywhere, the optical mode can be regarded as an incoherent statistical mixture of two states with different amplitudes and non-Gaussian fluctuations. As the driving power z increases from z_- to z_+ , the relative weights of the lobes continuously change from the lower branch to the upper one, describing the shift in probability for the system to be found in one or the other. This effect is robust to finite temperature of the mechanical environment.

The particular situation where the two stable branches are approximately equally likely ($z \simeq 0.26$ for $k_B T = \omega_m$) would enable the observation of noise-induced switching between both branches [57, 58] and constitute a clear signature of the nonlinear interaction between the optical and mechanical mode.

At higher driving power, $z > z_+$, when the MFEs have only one solution, both the optomechanical system and the Kerr medium exhibit sub-Poissonian statistics, $g^{(2)}(0) < 1$. Photon blockade in optomechanical systems has already been

predicted for $\chi > 1$ [9]. In our case, photon blockade is not very pronounced: we chose $\chi \ll 1$ to have bistable mean-field solutions that are appreciably distant in phase space. For the parameters of Fig. 4, this effect is slightly suppressed even further due to the finite-temperature bath, $n_{\text{th}} > 0$.

At various points of the paper, we have already demonstrated that the optomechanical system can be regarded as an effective Kerr medium in some range of parameters that we have specified. In particular, in the present section we have shown numerically that both systems exhibit the same features. For example, the photon number and the second-order photon correlation function follow the same parameter dependence, the Wigner function has a two-lobe structure, and both systems show photon blockade. As a further strong confirmation of this equivalence, we compare the states $\hat{\rho}_{\text{opt}}$ and $\hat{\rho}_K$ of the optical field in both systems. As can be seen in inset (c) of Fig. 4, their overlap F is close to 1 even at a finite thermal occupation of the mechanical mode. All of these calculations clearly establish the equivalence of the optomechanical system and a Kerr medium in the appropriate parameter range.

V. CONCLUSION

The mean-field equations for the optical mode of a dispersively coupled optomechanical system agree with those of a Kerr medium, a paradigmatic quantum optics system whose nonlinearity induces optical bistability. This raises the question of whether and under which conditions the two systems can be considered to be equivalent. We have therefore compared the optical bistability in an optomechanical system and a Kerr medium. A stability analysis of the mean-field solutions reveals differences between the two systems: the upper branch of an optomechanical system can become unstable due to position fluctuations of the mechanical degree of freedom. We have identified the regime of parameters where the two systems are equivalent. Corroborating this semiclassical approach, we have shown that the (optical) quantum steady states of both systems, obtained numerically, show large overlap. Our results clarify when an optomechanical system can be used as a Kerr nonlinearity in applications of quantum optics and quantum information.

ACKNOWLEDGEMENTS

We would like to thank D. Vitali for interesting discussions. This work was financially supported by the Swiss NSF, the NCCR Nanoscience, and the NCCR Quantum Science and Technology.

[1] J. L. O'Brien, A. Furusawa, and J. Vuckovic, *Nature Photon.* **3**, 687 (2009).

[2] P. Kok, W. J. Munro, K. Nemoto, T. C. Ralph, J. P. Dowling, and G. J. Milburn, *Rev. Mod. Phys.* **79**, 135 (2007).

[3] G. J. Milburn, *Phys. Rev. Lett.* **62**, 2124 (1989).

- [4] I. L. Chuang and Y. Yamamoto, *Phys. Rev. Lett.* **76**, 4281 (1996).
- [5] I. L. Chuang and Y. Yamamoto, *Phys. Rev. A* **52**, 3489 (1995).
- [6] S. L. Braunstein and P. van Loock, *Rev. Mod. Phys.* **77**, 513 (2005).
- [7] M. Aspelmeyer, T. J. Kippenberg, and F. Marquardt, (2013), [arXiv:1303.0733](https://arxiv.org/abs/1303.0733).
- [8] A. Nunnenkamp, K. Børkje, and S. M. Girvin, *Phys. Rev. Lett.* **107**, 063602 (2011).
- [9] P. Rabl, *Phys. Rev. Lett.* **107**, 063601 (2011).
- [10] I. Wilson-Rae, N. Nooshi, W. Zwerger, and T. J. Kippenberg, *Phys. Rev. Lett.* **99**, 093901 (2007).
- [11] F. Marquardt, J. P. Chen, A. A. Clerk, and S. M. Girvin, *Phys. Rev. Lett.* **99**, 093902 (2007).
- [12] C. M. Caves, *Phys. Rev. D* **23**, 1693 (1981).
- [13] V. Braginsky, F. Khalili, and K. Thorne, *Quantum Measurement* (Cambridge University Press, 1995).
- [14] K. Børkje, A. Nunnenkamp, B. M. Zwickl, C. Yang, J. G. E. Harris, and S. M. Girvin, *Phys. Rev. A* **82**, 013818 (2010).
- [15] T. P. Purdy, R. W. Peterson, and C. A. Regal, *Science* **339**, 801 (2013).
- [16] A. Kronwald, M. Ludwig, and F. Marquardt, *Phys. Rev. A* **87**, 013847 (2013).
- [17] S. Mancini, V. I. Man'ko, and P. Tombesi, *Phys. Rev. A* **55**, 3042 (1997).
- [18] S. Bose, K. Jacobs, and P. L. Knight, *Phys. Rev. A* **56**, 4175 (1997).
- [19] J. Qian, A. A. Clerk, K. Hammerer, and F. Marquardt, *Phys. Rev. Lett.* **109**, 253601 (2012).
- [20] V. Braginsky, M. Gorodetsky, and V. Ilchenko, *Physics Letters A* **137**, 393 (1989).
- [21] A. E. Fomin, M. L. Gorodetsky, I. S. Grudinin, and V. S. Ilchenko, *J. Opt. Soc. Am. B* **22**, 459 (2005).
- [22] F. Marino and F. Marin, *Phys. Rev. E* **83**, 015202 (2011); *Phys. Rev. E* **87**, 052906 (2013).
- [23] C. Fabre, M. Pinard, S. Bourzeix, A. Heidmann, E. Giacobino, and S. Reynaud, *Phys. Rev. A* **49**, 1337 (1994); S. Mancini and P. Tombesi, *Phys. Rev. A* **49**, 4055 (1994).
- [24] R. Ghobadi, A. R. Bahrapour, and C. Simon, *Phys. Rev. A* **84**, 033846 (2011).
- [25] A. Dorsel, J. D. McCullen, P. Meystre, E. Vignes, and H. Walther, *Phys. Rev. Lett.* **51**, 1550 (1983).
- [26] A. Gozzini, F. Maccarrone, F. Mango, I. Longo, and S. Barbarino, *J. Opt. Soc. Am. B* **2**, 1841 (1985).
- [27] P. D. Drummond and D. F. Walls, *J. Phys. A* **13**, 725 (1980).
- [28] D. Walls and G. Milburn, *Quantum Optics*, 2nd ed. (Springer, 2008).
- [29] A. A. Clerk, M. H. Devoret, S. M. Girvin, F. Marquardt, and R. J. Schoelkopf, *Rev. Mod. Phys.* **82**, 1155 (2010).
- [30] P. Meystre, E. M. Wright, J. D. McCullen, and E. Vignes, *J. Opt. Soc. Am. B* **2**, 1830 (1985).
- [31] P. Meystre and M. Sargent, *Elements of Quantum Optics* (Springer, 2007).
- [32] H. Risken, C. Savage, F. Haake, and D. F. Walls, *Phys. Rev. A* **35**, 1729 (1987); K. Vogel and H. Risken, *Phys. Rev. A* **39**, 4675 (1989).
- [33] F. Marquardt, J. G. E. Harris, and S. M. Girvin, *Phys. Rev. Lett.* **96**, 103901 (2006).
- [34] M. Ludwig, B. Kubala, and F. Marquardt, *New Journal of Physics* **10**, 095013 (2008).
- [35] In Refs. 36–38, similar criteria have been obtained using a quantum Brownian motion approach to treat mechanical dissipation. Their criteria are equivalent to $c_{1,2}$ in the limit $Q_m \gg 1$.
- [36] C. Genes, A. Mari, P. Tombesi, and D. Vitali, *Phys. Rev. A* **78**, 032316 (2008).
- [37] D. Vitali, S. Gigan, A. Ferreira, H. R. Böhm, P. Tombesi, A. Guerreiro, V. Vedral, A. Zeilinger, and M. Aspelmeyer, *Phys. Rev. Lett.* **98**, 030405 (2007); D. Vitali, P. Tombesi, M. J. Woolley, A. C. Doherty, and G. J. Milburn, *Phys. Rev. A* **76**, 042336 (2007).
- [38] C. Genes, D. Vitali, P. Tombesi, S. Gigan, and M. Aspelmeyer, *Phys. Rev. A* **77**, 033804 (2008).
- [39] Our treatment neglects other possible nonlinear effects that could preclude the observation of instability in the upper branch. In particular, photothermal forces have proven important in experiments with silica microcavities as reported in Ref. 59.
- [40] C. A. Regal, J. D. Teufel, and K. W. Lehnert, *Nat. Phys.* **4**, 555 (2008).
- [41] T. Rocheleau, T. Ndukum, C. Macklin, J. B. Hertzberg, A. A. Clerk, and K. C. Schwab, *Nature* **463**, 72 (2010).
- [42] J. D. Teufel, D. Li, M. S. Allman, K. Cicak, A. J. Sirois, J. D. Whittaker, and R. W. Simmonds, *Nature* **471**, 204 (2011).
- [43] F. Massel, T. T. Heikkilä, J.-M. Pirkkalainen, S. U. Cho, H. Saloniemi, P. J. Hakonen, and M. A. Sillanpää, *Nature* **480**, 351 (2011).
- [44] S. Groblacher, K. Hammerer, M. R. Vanner, and M. Aspelmeyer, *Nature* **460**, 724 (2009).
- [45] J. Chan, T. P. M. Alegre, A. H. Safavi-Naeini, J. T. Hill, A. Krause, S. Groblacher, M. Aspelmeyer, and O. Painter, *Nature* **478**, 89 (2011).
- [46] Y.-S. Park and H. Wang, *Nat. Phys.* **5**, 489 (2009).
- [47] A. Schliesser, R. Riviere, G. Anetsberger, O. Arcizet, and T. J. Kippenberg, *Nat. Phys.* **4**, 415 (2008).
- [48] E. Verhagen, S. Deléglise, S. Weis, A. Schliesser, and T. Kippenberg, *Nature* **482**, 63 (2012).
- [49] K. W. Murch, K. L. Moore, S. Gupta, and D. M. Stamper-Kurn, *Nat. Phys.* **4**, 561 (2008).
- [50] M. H. Schleier-Smith, I. D. Leroux, H. Zhang, M. A. Van Camp, and V. Vuletić, *Phys. Rev. Lett.* **107**, 143005 (2011).
- [51] D. W. C. Brooks, T. Botter, S. Schreppler, T. P. Purdy, N. Brahms, and D. M. Stamper-Kurn, *Nature* **488**, 476 (2012).
- [52] J. D. Thompson, B. M. Zwickl, A. M. Jayich, F. Marquardt, S. M. Girvin, and J. G. E. Harris, *Nature* **452**, 72 (2008).
- [53] O. Arcizet, P.-F. Cohadon, T. Briant, M. Pinard, and A. Heidmann, *Nature* **444**, 71 (2006).
- [54] D. Kleckner, B. Pepper, E. Jeffrey, P. Sonin, S. M. Thon, and D. Bouwmeester, *Opt. Express* **19**, 19708 (2011).
- [55] F. Mueller, S. Heugel, and L. J. Wang, *Phys. Rev. A* **77**, 031802 (2008).
- [56] K. Vogel and H. Risken, *Phys. Rev. A* **42**, 627 (1990).
- [57] M. Rigo, G. Alber, F. Mota-Furtado, and P. F. O'Mahony, *Phys. Rev. A* **55**, 1665 (1997).
- [58] J. Kerckhoff, M. A. Armen, and H. Mabuchi, *Opt. Express* **19**, 24468 (2011).
- [59] O. Arcizet, R. Rivière, A. Schliesser, G. Anetsberger, and T. J. Kippenberg, *Phys. Rev. A* **80**, 021803 (2009).